# Temporal dependence of cysteine protease activation following excitotoxic hippocampal injury

**Jennifer N. Berry**, **Lynda Sharrett-Field**, **Tracy R. Butler**, and **Mark A. Prendergast**
Department of Psychology, Spinal Cord and Brain Injury Research Center, B449 Biomedical and Biological Sciences Research Building, 741 S. Limestone St., Lexington, KY 40536-0509

## Abstract

Excitotoxic insults can lead to intracellular signaling cascades that contribute to cell death, in part by activation of proteases, phospholipases, and endonucleases. Cysteine proteases, such as calpains, are calcium-activated enzymes which degrade cytoskeletal proteins, including microtubule-associated proteins, tubulin, and spectrin, among others. The current study used the organotypic hippocampal slice culture model to examine whether pharmacologic inhibition of cysteine protease activity inhibits *N*-methyl-D-aspartate- (NMDA-) induced excitotoxic (20 μM NMDA) cell death and changes in synaptophysin immunoreactivity. Significant NMDA-induced cytotoxicity (as measured by propidium iodide [PI] uptake) was found in the CA1 region of the hippocampus at all timepoints examined (24, 72, 120 hours), an effect significantly attenuated by co-exposure to the selective NMDA receptor antagonist DL-2-amino-5-phosphonopentanoic acid (APV), but not MDL-28170, a potent cysteine protease inhibitor. Results indicated sparing of NMDA-induced loss of the synaptic vesicular protein synaptophysin in all regions of the hippocampus by MDL-28170, though only at early timepoints after injury. These results suggest calcium-dependent recruitment of cysteine proteases within 24 hours of excitotoxic insult, but activation of alternative cellular degrading mechanisms after 24 hours. Further, these data suggest that synaptophysin may be a substrate for calpains and related proteases.

### Keywords

NMDA receptors; excitotoxicity; synaptophysin; cysteine protease; calpain

---

Excitotoxicity is the overexcitation of neurons due to the excessive activation of excitatory amino acid (EAA) receptors and likely contributes to central nervous system injury in neurodegenerative states, including traumatic brain injury (TBI), ischemia, stroke, epilepsy, and amyotrophic lateral sclerosis (see Choi, 1992 for a review). Calcium ($Ca^{2+}$)-permeable glutamatergic *N*-methyl-D-aspartate (NMDA) receptors are thought to be an integral component of the excitotoxic cascade. For example, Choi et al. reported that co-exposure to the competitive NMDA receptor antagonist 2-amino-7-phosphovaleric acid (APV) attenuated NMDA- and glutamate- excitotoxicity in primary cortical cell cultures (Choi et al., 1988), while antagonists of AMPA or kainate-type glutamate receptors did not. Neurons maintain low intracellular $Ca^{2+}$ concentrations, as compared to extracellular space, by

regulating $Ca^{2+}$ efflux, intracellular $Ca^{2+}$ buffering, and intracellular $Ca^{2+}$ storage (Sattler and Tymianski, 2000). Although small, physiologically relevant amounts of $Ca^{2+}$ are necessary for the cell to function properly, excessive $Ca^{2+}$ influx, such as that seen during a state of neural hyperexcitability, may quench regulatory mechanisms and initiate cytotoxicity associated with activity of proteases, phospholipases, and endonucleases (Choi, 1995; Sattler and Tymianski, 2000) or alterations in mitochondrial bioenergetics (for a review, see Pivovarova and Andrews, 2010).

Cysteine proteases, such as calpains, are $Ca^{2+}$-activated enzymes that degrade cytoskeletal proteins, including microtubule-associated proteins, tubulin, and spectrin, among others (Siman and Noszek, 1988; Vosler et al., 2008). Siman and colleagues (1989) reported that EAA-induced calpain I activation is closely associated with EAA-induced hippocampal damage since only those doses of intraventricular-administrated EAAs which produce hippocampal damage also resulted in calpain I activation. Further, calpain inhibition with use of the cysteine protease inhibitor MDL-28170 was found to be neuroprotective when given either as a pretreatment or immediately following a glutamate challenge in primary hippocampal cultures (Rami et al., 1997). Gellerman et al. (1997) reported that loss of GluR1 subunits in the hippocampus following NMDA exposure was prevented by co-exposure to calpain inhibitor I or calpeptin. One recent study reported that both NMDA and non-NMDA glutamate receptor agonism activated calpain as reflected in accumulation of spectrin breakdown products; however, only the NMDA receptor antagonist was effective at reducing glutamate-induced toxicity (Del Rio et al., 2008). These breakdown products have been detected *in vitro* following as little as a 5 minute exposure to NMDA (Bahr et al., 1995), while *in vivo* work has suggested that spectrin breakdown takes hours or days to be observed following NMDA-induced neurodegeneration (Siman et al., 1989). Previous research has also indicated that calpain-dependent axonal varicosities appear prior to neuronal damage following glutamate-induced excitotoxic insult (Hou et al., 2009). Thus, there has been confusion regarding which markers might reflect calpain-mediated cell death and the timecourse associated with the expression of these markers remains unclear. Vosler et al. (2008) describe evidence for the existence of more than sixty calpain substrates in neurodegeneration.

Several notable constituents of the cytoskeleton, including the vesicle protein synaptophysin, are not clearly defined as calpain substrates. Research examining the possibility that synaptophysin may be a substrate for calpain and related proteases has yielded contradictory results (Thompson et al., 2006; Lee et al., 2008). Synaptophysin is a synaptic vesicle protein found in the axon terminal of presynaptic neurons and has been shown to be present in the brain and spinal cord (Wiedenmann and Franke, 1985). Synaptophysin is thought to be involved in the docking and fusion of the vesicle with the plasma membrane (Sudhof, 1995) and has been implicated in synaptogenesis and synaptic reorganization (Bergmann et al., 1997). Accordingly, synaptophysin has been used to assess the integrity of axon terminals in a number of injury paradigms, including glutamate-induced excitotoxicity (Lee et al., 2008), TBI (Thompson et al., 2006), and ischemia (Stroemer et al., 1995).

The present studies employed the organotypic hippocampal cell culture model to examine the temporal and topographical nature of NMDA exposure and cysteine protease activity on neuronal viability and synaptophysin abundance. The organotypic model has been shown to closely mimic *in vivo* structural and functional integrity over time and serves as a sensitive model of NMDA receptor-mediated effects on neuronal viability (Gutierrez and Heinemann, 1999; Martens and Wree, 2001). The temporal and topographical characterization of cellular injury or death following EAA receptor activation may be particularly important in further identifying novel substrates, such as synaptophysin, for calpain and other cysteine proteases

in excitotoxic neurodegeneration. Further, it was hypothesized that the effects associated with NMDA receptor overactivation will be more pronounced in the CA1 region of the hippocampus in accordance with previous reports (Butler et al., 2010).

## EXPERIMENTAL PROCEDURES

### Organotypic Hippocampal Slice Culture Procedure

Eight day old male and female Spraque-Dawley rats (acquired from Harlan Laboratories; Indianapolis, IN) were humanely sacrificed and the brains were aseptically removed. Following removal, brains were transferred into ice-cold dissecting media, composed of Minimum Essential Medium (MEM; Invitrogen, Carlsbad, CA), 25 mM HEPES (Sigma, St. Louis, MO), and 50 $\mu$M streptomycin/penicillin (Invitrogen). Bilateral hippocampi were removed in whole and cleaned of extra tissue under a dissecting microscope. Hippocampi were then placed into culture media, which contains dissecting medium along with distilled water, 36 mM glucose (Fisher, Pittsburgh, PA), 25% Hanks' Balanced Salt Solution (Invitrogen), 25% (v/v) heat-inactivated horse serum (Sigma), and 0.05% streptomycin/ penicillin. Unilateral hippocampi were sectioned at 200 $\mu$m using a McIllwain Tissue Chopper (Mickle Laboratory Engineering Co. Ltd., Gomshall, UK). Following sectioning, three intact hippocampal slices were plated onto a Millicell-CM 0.4 $\mu$m biopore membrane insert with 1 mL of pre-incubated culture media added to the bottom of each well of a six well plate, yielding a total of 18 intact slices per plate. Excess culture medium was aspirated from the top of each well and the plates were then incubated at 37°C with a gas composition of 5% $CO_2$/95% air for 5 days to allow tissue to affix to the Teflon membrane. Care of all animals was carried out in agreement with the National Institutes of Health Guide for the Care and Use of Laboratory Animals (NIH Publications No. 80–23, revised 1996) and the University of Kentucky's Institutional Animal Care and Use Committee.

### Drug Exposure

At 5 days *in vitro*, slices were randomly transferred to new culture plates containing either 1 mL of culture media containing propidium iodide (PI; 3.74 $\mu$M; Molecular Probes, Eugene, OR) or 1 mL of culture media containing PI and the following drugs: NMDA (20 $\mu$M; Sigma); MDL-28170 (2.5 or 25$\mu$M; Sigma); NMDA + MDL-28170 (as above); APV (50 $\mu$M; Sigma); or NMDA + APV (as above) dissolved in 1 mL of culture media. MDL-28170 was first dissolved in dimethyl sulfoxide (DMSO; Fisher) to yield a final concentration of 0.5% DMSO in culture media. Thus, an additional group of slices was exposed to only 0.5% DMSO. For studies involving MDL-28170, cultures were first exposed to MDL-28170 or culture media two hours prior to the addition of NMDA. PI is a nucleic acid stain used to detect cell damage and was used to measure cytotoxicity as described below. All experiments were replicated at least twice, with each experimental condition (treatment X exposure time X sex within region) containing n=18–27 slices. A total of 14 rats litters were used for these experiments.

### Cytotoxicity assessment

Previous work has shown that PI reliably correlates with other measures of cell death (for a review, see Zimmer et al., 2000), and as such was used as a measure of cytotoxicity in the present studies (i.e. staining of neurons and glia with compromised membranes). PI was measured in the granule cell layer of the dentate gyrus (DG) as well as in the pyramidal cell layers of the cornu ammonis 3 (CA3) and the cornu ammonis 1 (CA1) regions of the hippocampal formation using fluorescent microscopy. Slices were visualized with SPOT advanced version 4.0.2 software for Windows (W. Nuhsbahm Inc.; McHenry, IL, USA) using a 5× objective with a Leica DMIRB microscope (W. Nuhsbahm Inc.; McHenry, IL, USA) fitted for fluorescence detection (mercury-arc lamp) using blue-green light and

connected to a personal computer through a SPOT 7.2 color mosaic camera (W. Nuhsburg Inc.; McHenry, IL, USA). PI has an emission wavelength of 620 nm in the visual range and a peak excitation wavelength of 536 nm and was excited using a band-pass filter which excites a range of wavelengths (510–560 nm). Densitometry using Image J software (National Institutes of Health, Bethesda, MD) was used to measure the intensity of PI fluorescence within each hippocampal region. A background measurement was taken from the visual field surrounding each slice and was subsequently subtracted from the regional measurement from each slice. Within each region, raw measurements of PI uptake were converted to percent control before statistical analysis to control for potential differences between rat litters used for separate replications.

## Immunohistochemical Analysis of Synaptophysin

At 24, 72, or 120 hours following the initiation of NMDA exposure, tissue slices were imaged once for cytotoxicity (PI uptake) and subsequently fixed to assess synaptophysin immunoreactivity by transferring the hippocampal slice insert to a plate containing 1 mL of 10% formalin solution on the bottom of each well. One mL of formalin was also placed on top of the insert and the plates were allowed to sit for 30 minutes. The slices were then washed carefully (1 mL on bottom of the well and 1 mL on top of the well) with 1 X phosphate buffered saline (PBS) twice and stored with 1 mL of 1 X PBS on the bottom of the well overnight at 4°C. Following overnight storage, the inserts were transferred to a plate containing 1 mL of membrane permeabilization buffer (200 mL 1 X PBS (Invitrogen), 200 μL Triton X-100 (Sigma), 0.010 mg Bovine Serum (Sigma)) in each well and 1 mL of permeabilization buffer was also placed on top of each insert containing the slices. The slices were allowed to sit in buffer for 45 minutes to allow the buffer to penetrate the slice and were then washed twice with 1 X PBS as described earlier. Inserts were then transferred to a plate containing 1 mL of 1 X PBS on the bottom of each well and were treated with 1 mL of permeabilization buffer containing mouse anti-synaptophysin (1:200; Sigma) on top of each well. Plates were then stored at 4°C for 24 hours. Following 24 hours, the slices were washed gently with 1 X PBS twice and were again transferred to a plate containing 1 mL of 1 X PBS on bottom. At this point, slices were treated with 1 mL of permeabilization buffer containing the goat anti-mouse secondary antibody conjugated to fluorescein isothiocyanate (FITC; 1:100; Sigma) on top of the insert and were stored at 4°C for 24 hours. After 24 hours, slices were washed twice with 1 X PBS as described previously and placed into a plate containing 1 mL of 1 X PBS on the bottom of each well. The slices were imaged immediately with PBS under each insert.

The slices were visualized as described previously above (see cytotoxicity assessment) except that the secondary antibody with FITC was excited using a band-pass filter at 495 nm (520 nm emission). Densitometry using Image J software (National Institutes of Health, Bethesda, MD) was used to measure the intensity of the FITC fluorescence. A background measurement of fluorescence was taken from the visual field surrounding each slice and was subsequently subtracted from the region measurement of each slice before analysis. The intensity was measured in each of the three regions of interest: the granule cell layer of the dentate gyrus and the pyramidal cell layers of the CA3 and CA1 regions of the hippocampus. To control for the variability between each replication, measurements of FITC immunoreactivity were converted to percent control for each region before statistical analysis.

## Statistical analyses

Each experiment was conducted a minimum of 2 times using different rat litters. Data from each replication were converted into percent control values, yielding 18–27 slices per treatment group (drug treatment X exposure time X sex within each region). Previous

studies have shown a differential vulnerability to NMDA toxicity among the regions of the hippocampus, with the CA1 region being the most vulnerable to excitotoxic insult (Butler et al., 2010). For experiments examining the effects of NMDA and APV on PI uptake and synaptophysin immunoreactivity, a three-way ANOVA was conducted within each region with the following factors: treatment (control, NMDA alone, APV alone, NDMA+APV co-exposure) X time (24, 72, 120 hours) X sex (male, female). For studies investigating the effects of NMDA and MDL-28170 on PI uptake and synaptophysin immunoreactivity, a three-way ANOVA was also conducted for each region, with the following factors: treatment (DMSO, MDL-28170, NMDA+DMSO, NMDA+MDL-28170 co-exposure) X time (24, 72, 120 hours) X sex (male, female). All treatment groups were compared to the time-appropriate control condition. If sex differences were not observed, data derived from male and female hippocampi were combined and two-way ANOVAs were performed. When appropriate, post-hoc tests were conducted using Fisher's LSD to examine further effects. Statistical significance was set at $p < 0.05$.

## RESULTS

### Basal Uptake of Propidium Iodide and Synaptophysin Immunoreactivity

Initial studies examined the unstimulated uptake of PI from medium and synaptophysin immunoreactivity in NMDA-naïve explants. As no sex differences were observed in the initial analysis, data were collapsed across sex. With regard to levels of PI uptake in control slices, a significant interaction between region and exposure time was found (Figure 1A; $F_{(4, 315)} = 17.571$, $p < 0.001$). In the CA1 pyramidal and DG granule cell layers, PI uptake following 120 hours was significantly greater than that following either 24 or 72 hours. At the 24 and 72 hour timepoints, PI uptake was greatest in the pyramidal cell layer of the CA3 regions, as compared to the pyramidal layer of the CA1 region or the granule cell layer of the DG. At the 120 hour timepoint, the CA1 pyramidal cell layer was found to have the greatest PI uptake as compared to either the CA3 or the DG (Figure 1A). With regard to synaptophysin immunoreactivity, a two-way ANOVA revealed a significant interaction between region and exposure time (Figure 1B; $F_{(4, 315)} = 10.161$, $p < 0.001$). Interestingly, synaptophysin immunoreactivity increased markedly in each cell layer of the hippocampal formation with *in vitro* aging. Synaptophysin immunoreactivity following 120 hour exposure was significantly greater than that seen following either 72 or 24 hour exposure in all regions of the hippocampal formation. Further, within the CA1 region only, the raw value of synaptophysin immunoreactivity following 72 hour exposure was significantly greater than that seen following 24 hour exposure. At each timepoint, the CA1 pyramidal cell layer had significantly greater levels of synaptophysin immunoreactivity than the pyramidal cell layer of the CA3 region or granule cells of the DG. In sum, these findings demonstrate that pyramidal cells of the CA1 and CA3 regions show the greatest level of PI uptake and that the CA1 region has the greater level of synaptophysin immunoreactivity, though increased immunoreactivity was observed in each region with aging *in vitro*.

### NMDA-Induced Cytotoxicity

Additional studies were conducted to assess the time-dependent effects of exposure to NMDA and the competitive NMDA receptor antagonist APV on PI uptake at 24, 72, and 120 hours. There was no difference in toxicity between sexes within each treatment group, and male and female data were combined for further analysis. Thus, a two-way ANOVA (treatment X exposure time) within each region was conducted. A significant interaction between treatment and exposure time was observed in the pyramidal cell layer of the CA1 region (Figure 2A; $F_{(6, 420)} = 30.842$, $p < 0.001$). Exposure to NMDA produced a significant time-dependent increase in PI uptake compared to control cultures, while the addition of APV significantly attenuated this increase (Fisher's LSD post-hoc, $p < 0.05$). The most robust

NMDA-induced PI uptake was seen at the 24 hour timepoint (~375% control) while a smaller, yet still significant, increase in PI uptake was seen at the 72 and 120 hour timepoints (~290% and 198% control, respectively; post-hoc, $p < 0.05$). Co-exposure to APV significantly attenuated the toxicity observed at each time point. Exposure to APV alone produced no significant changes in toxicity in NMDA-naïve tissue at any timepoint (data not shown).

Significant main effects of treatment (Figure 2B; $F(3, 420=14.80$, $p < 0.001$) and exposure time ($F(2, 420=3.173$, $p < 0.05$) were observed in the pyramidal cell layer of the CA3 region. Modest (~115% control), though significant, increases in PI uptake were found in cultures exposed to NMDA when collapsed across time (post-hoc, $p < 0.05$). Collapsed across time, these effects were not significantly attenuated by APV co-exposure. Exposure to APV alone produced no significant changes in toxicity in NMDA-naïve tissue in the CA3 region (data not shown). Post-hoc analysis of the main effect of time demonstrated that PI uptake following either 24 or 72 hour exposure was significantly greater than PI uptake following 120 hour exposure (data not shown; post-hoc, $p < 0.05$).

In the granule cell layer of the DG, only a significant main effect of treatment was observed (Figure 2C; $F(3, 420)=23.367$, $p < 0.001$). Collapsed across time, exposure to NMDA resulted in a significant increase (~125% control) in PI uptake, an effect that was significantly attenuated by co-exposure with APV (post-hoc, $p < 0.05$). Exposure to APV alone produced no significant changes in toxicity in NMDA-naïve tissue in the DG region (data not shown). Representative images of these effects are presented in Figure 2D.

## NMDA-Induced Loss of Synaptophysin

No significant sex differences were observed in the pyramidal cell layer of the CA1, therefore male and female were combined for a two-way ANOVA (treatment X exposure time). A significant interaction in this region was observed (Figure 3A; $F(6, 420)=5.347$, $p < 0.001$). At each timepoint examined, NMDA exposure resulted in a loss of synaptophysin immunoreactivity (for example, more than a 50% reduction was observed at 120 hours). The addition of APV blocked this NMDA-induced effect (post-hoc, $p < 0.05$). This NMDA-induced decrease in synaptophysin immunoreactivity within the CA1 was time-dependent, such that longer exposure (i.e. 72 or 120 hour) produced a significantly greater deficit (42% control and 32% control, respectively) in synaptophysin immunoreactivity compared to shorter exposure (i.e. 24 hour; 72% control). Exposure to APV alone produced no significant changes in synaptophysin immunoreactivity in NMDA-naïve tissue at any timepoint (data not shown).

In the pyramidal cell layer of the CA3 region, significant main effects of both exposure time ($F(3,420)=5.681$, $p < 0.001$) and treatment (Figure 3B; $F(2, 420)=7.396$, $p < 0.001$) were observed. Collapsed across exposure time, treatment with NMDA resulted in a significant decrease (84% control) in synaptophysin immunoreactivity in the pyramidal cell layer as compared to control cultures. The loss of synaptophysin immunoreactivity was significantly attenuated by co-exposure of to APV. Compared to control cultures, exposure to APV alone produced no significant changes in synaptophysin immunoreactivity in NMDA-naïve tissue in the CA3 region (data not shown). Further, data collapsed across treatment revealed that synaptophysin immunoreactivity at 120 hours was significantly lower than that at 24 or 72 hours (data not shown).

A significant main effect of treatment (Figure 3C; $F(3,420)=16.169$, $p < 0.001$) was observed in the granule cell layer of the DG. Collapsed across exposure time, treatment with NMDA resulted in a significant decrease (73% of control levels) in synaptophysin immunoreactivity in the DG region of the hippocampus as compared to control cultures. The loss of

synaptophysin immunoreactivity in the DG following NMDA exposure, collapsed across time, was significantly attenuated by co-exposure to APV. Compared to control cultures, exposure to APV alone produced no significant changes in synaptophysin immunoreactivity in NMDA-naïve tissue (data not shown). Representative images of hippocampal slices labeled with synaptophysin are presented in Figure 3D.

**Effect of MDL-28170 on NMDA-induced toxicity and loss of synaptophysin**

A final series of studies examined the role that cysteine protease activation may have in promoting the cytotoxicity observed following NMDA exposure. Similar to the findings above, no sex differences were observed following an initial three-way ANOVA, thus data were collapsed across sex. In the pyramidal cell layer of the CA1 region, a significant interaction of treatment X exposure time was found (Figure 4A; $F_{(10, 630)}=86.391$, $p<0.001$). Similar to previously presented data, co-exposure to NMDA and vehicle (DMSO) produced time-dependent increases in cytotoxicity in the CA1 region compared to vehicle alone (post-hoc, $p<0.05$), while co-exposure to MDL-28170 (2.5 or 25 $\mu$M) did not reduce NMDA-induced toxicity at any timepoint. No effect was observed with MDL-28170 alone compared to vehicle control cultures in NMDA-naïve tissue at any timepoint (data not shown).

In the pyramidal cell layer of the CA3 region, a significant interaction of treatment X exposure time was observed (Figure 4B; $F_{(10, 630)}=9.599$, $p<0.001$). Co-exposure to NMDA and DMSO resulted in significantly increased PI uptake as compared to vehicle control cultures at 24 and 120, but not 72, hours (post-hoc, $p<0.05$). NMDA-induced toxicity was not prevented by the co-exposure to MDL-28170 (2.5 or 25 $\mu$M) at any timepoint, as NMDA+MDL resulted in significant toxicity at all timepoints examined. There was no difference in PI uptake in NMDA-naïve tissue treated with MDL-28170 alone compared to vehicle controls (data not shown).

Within the DG granule cell layer, a significant interaction of treatment X exposure time was also found (Figure 4C; $F_{(10, 630)}=13.734$, $p<0.001$). Co-exposure to NMDA and DMSO for 24 hours significantly increased PI uptake as compared to vehicle-treated cultures, an effect which was not significantly attenuated by co-exposure to MDL-28170 (2.5 or 25 $\mu$M) and NMDA. Further, co-exposure to NMDA and MDL-28170 resulted in slight, but significant, increases in PI uptake at 72 and 120 hours compared to vehicle-treated cultures. Exposure to MDL-28170 alone in NMDA-naïve tissue produced a slight, but significant, increase in PI uptake following 72, but not 24 or 120, hours ($134.383\pm7.917$ versus $100\pm4.275$ for vehicle controls, $p<0.05$; data not shown). Representative images of hippocampal slices labeled with PI are presented in Figure 4D.

Following analysis of PI uptake, cultures were subsequently formalin-fixed to examine the immunoreactivity of the synaptic vesicle protein synaptophysin. Sex differences were not observed with use of an initial three-way ANOVA, thus male and female data were combined for further two-way analyses. In the pyramidal cell layer of the CA1 region, a significant interaction of treatment X exposure time was found (Figure 5A; $F_{(10, 630)}=8.602$, $p<0.001$). Co-exposure to NMDA and DMSO caused a time-dependent loss of synaptophysin immunoreactivity compared to vehicle-treated cultures at all timepoints examined. These effects were blocked by co-exposure to NMDA+MDL-28170 (25 $\mu$M) though, interestingly, only at the early timepoints. MDL-28170 co-exposure significantly attenuated the NMDA-induced loss of synaptophysin immunoreactivity at 24 and 72 hours, though not up to vehicle-treated control levels at 72 hours. Exposure to MDL-28170 alone in NMDA-naïve tissue produced a significant increase in synaptophysin immunoreactivity following 72, but not 24 or 120, hours in the CA1 region of the hippocampus ($137.910\pm7.757$ versus $100\pm4.755$ for vehicle controls, $p<0.05$; data not shown).

In the pyramidal cell layer of the CA3 region, significant main effects of both treatment (Figure 5B; $F_{(5,630)}=17.247$, $p<0.001$) and exposure time ($F_{(2,630)}=7.746$, $p<0.001$) were observed. Collapsed across exposure time, treatment with NMDA+DMSO resulted in a significant decrease (82% vehicle control) in synaptophysin immunoreactivity compared to vehicle-treated cultures. The loss of synaptophysin immunoreactivity was significantly attenuated by co-exposure to MDL-28170 (25 $\mu$M; 102% vehicle control). Similar to data from the CA1, NMDA-naïve cultures exposed to MDL-28170 had significantly increased synaptophysin immunoreactivity compared to vehicle-treated cultures collapsed over time (124.804±4.786 versus 100±3.551 for vehicle controls, $p<0.001$; data not shown). Further, data collapsed across treatment revealed that synaptophysin immunoreactivity at 120 hours was significantly lower than that at 24 or 72 hours (data not shown).

A significant treatment X exposure time interaction was observed in the granule cell layer of the DG region (Figure 5C; $F_{(10,630)}=3.812$, $p<0.001$). NMDA+DMSO co-exposure produced a significant decrease in synaptophysin immunoreactivity as compared to vehicle-treated cultures at all timepoints examined (post-hoc, $p<0.05$). This effect was significantly blocked by co-exposure to NMDA and MDL-28170 (25 $\mu$M) at the 24 and 72 hour timepoints (post-hoc, $p<0.05$). However, co-exposure to NMDA and MDL-28170 was not protective against the NMDA-induced loss of synaptophysin at 120 hours. As observed in the CA1 region, exposure to MDL-28170 alone in NMDA-naïve tissue produced a significant increase in synaptophysin immunoreactivity following 72, but not 24 or 120, hours (131.460±6.787 versus 100±4.958 for vehicle controls, $p<0.001$; data not shown). Representative images of synaptophysin immunoreactivity in hippocampal slices are shown in Figure 5D.

Because the most robust effect of MDL-28170 in regards to protection against NMDA-induced synaptophysin immunoreactivity loss was found at 24 hours, a lower concentration of MDL-28170 (2.5 $\mu$M) was also examined at this timepoint. No sex differences were observed in any region following an initial two-way ANOVA of sex X treatment, thus data from each region were collapsed across sex. In the pyramidal cell layer of the CA1 region, a significant main effect of treatment was found (table 1; $F_{(3, 212)}=169.866$, $p<0.001$). Similar to previously presented data, co-exposure to NMDA (20 $\mu$M) and vehicle (DMSO) produced increases in cytotoxicity in the CA1 region compared to vehicle alone (post-hoc, $p<0.05$), while co-exposure to MDL-28170 (2.5 $\mu$M) did not reduce NMDA-induced toxicity. Main effects of treatment were also observed in the CA3 and DG regions ($F_{(3, 212)}=13.159$, $p<0.001$; $F_{(3, 212)}=18.560$, $p<0.001$, respectively). Similar to that observed in the CA1, data from the CA3 and DG regions indicate significant NMDA-induced toxicity following co-exposure to either NMDA+DMSO or NMDA+MDL-28170 at 2.5 $\mu$M (post-hoc, $p<0.05$). Thus, as with the higher concentration of MDL-28170 (25 $\mu$M), co-exposure to MDL-28170 (2.5 $\mu$M) did not prevent NMDA-induced cytotoxicity in any region.

Loss of synaptophysin immunoreactivity was also examined using a lower concentration of MDL-28170 at 24 hours only. As with PI data, no sex differences in synaptophysin immunoreactivity were observed in any region and data were subsequently collapsed across sex. A significant main effect of treatment was observed in the CA1 region (table 1; $F_{(3, 212)}=22.214$, $p<0.001$). Co-exposure to NMDA+DMSO resulted in a significant loss of synaptophysin immunoreactivity compared to vehicle-treated cultures (post-hoc, $p<0.05$). This effect was significantly attenuated by co-exposure to NMDA+MDL-28170 (2.5 $\mu$M; post-hoc, $p<0.05$). Main effects of treatment were also observed in the CA3 and DG regions ($F_{(3, 212)}=6.061$, $p<0.001$; $F_{(3, 212)}=7.836$, $p<0.001$, respectively). The NMDA+DMSO-induced loss of synaptophysin immunoreactivity failed to reach statistical significance in the CA3 region (~86% vehicle control cultures); however co-exposure to NMDA+MDL-28170 (2.5 $\mu$M) in this region resulted in synaptophysin immunoreactivity levels above vehicle-

treated cultures (107% vehicle control) and levels significantly above those seen following NMDA+DMSO. Similar to that observed in the CA1, data from the DG region indicates significant NMDA-induced toxicity following co-exposure to NMDA+DMSO (post-hoc, p<0.05), an effect which was significantly attenuated following co-exposure to MDL-28170 (2.5 μM). This lower concentration of MDL-28170 attenuated the NMDA-induced loss of synaptophysin immunoreactivity in each region of the hippocampus examined, though not to the extent that the higher concentration (25 μM) did in the CA1 region (~92% vehicle control for 2.5 μM vs. ~106% vehicle control for 25 μM). Similar to the effects observed with MDL-28170 25 μM in NMDA-naïve tissue, NMDA-naïve cultures exposed to MDL-28170 2.5 μM had slight, but significantly, increased synaptophysin immunoreactivity in each region of the hippocampus (~109% vehicle control in CA1 region; post-hoc, p<0.05; data not shown).

## DISCUSSION

Recent findings have demonstrated that pyramidal cells of the hippocampal formation, particularly those of the CA1 region, are uniquely sensitive to the excitotoxic effects of NMDA receptor activation, relative to granule cells of the DG (Prendergast et al., 2004; Butler et al., 2010). This increased sensitivity to the neurotoxic effects of NMDA itself is associated with an increase in the density of NR1 and NR2B subunits of the NMDA receptor in the pyramidal cell layer of organotypic hippocampal explants. In kind with these observations, analysis of PI uptake in untreated (i.e. NMDA-naïve) hippocampal explants demonstrated that the uptake of PI is greater in pyramidal cell layers than in the granule cell layer of the DG. This regional distinction in unstimulated PI uptake may be related to the excitotoxic effects of "medium-change," as previously observed in organotypic explants (Mayer et al., 2002) and dissociated neurons (Driscoll et al., 1993). Driscoll et al. (1993) demonstrated that *de novo* synthesis of extracellular glutamate in cell culture medium isolated from primary neuronal cell culture, even after several hours of isolation from cell cultures, was associated with accumulation of glutaminase in medium. Further, Mayer et al. (2002) demonstrated that treatment of organotypic hippocampal explants with the NMDA receptor antagonists acamprosate, MK-801, or ifenprodil significantly reduced the PI uptake associated with acute medium change; thus suggesting that medium-change toxicity is specifically related to NMDA receptor activation. Resistance to toxicity associated with medium change in the DG may be associated with the ability of granule cells to buffer accumulated $Ca^{2+}$ or with relative paucity of $Ca^{2+}$-sensitive downstream effectors. The DG granule cell layer possesses the greatest immunoreactivity of calbindin-D28K compared to either the CA1 or CA3 regions (Prendergast et al., 2001). Calbindin-D28K is a $Ca^{2+}$ binding protein which sequesters cytosolic $Ca^{2+}$ for a period of time, thus protecting the cell from $Ca^{2+}$-mediated cell death (for a review, see Baimbridge et al., 1992), such as that likely observed with excess NMDA receptor activation.

Immunoreactivity of the synaptic vesicle protein synaptophysin was greater in the CA1 pyramidal cell projection field than in the primary projection layers of the CA3 and DG. This is consistent with the findings of Butler et al. (2010) in demonstrating greater neuronal density in this subregion of the hippocampal formation, reflected in greater density of NeuN and MAP-2 immunoreactivity. It is intriguing that immunoreactivity of synaptophysin increased in a time-dependent manner by approximately two-fold as explants aged to 120 hours *in vitro*. However, this was observed only in the CA1 region pyramidal cell projection layer. Previous research has suggested that a synaptic reorganization occurs in the organotypic hippocampal slice culture model used in the present set of experiments and that this reorganization leads to the production of new synaptic pathways between the CA1 and DG (Gutierrez and Heinemann, 1999; Mulholland and Prendergast, 2003). Thus, the time-dependent increase in synaptophysin immunoreactivity in the projection layer of the CA1

region may suggest synaptogenesis with *in vitro* aging following disruption of the afferent innervation to the DG.

## NMDA-induced cytotoxicity

The present results demonstrate a time-dependent NMDA-induced increase in PI fluorescence within the CA1 region only, such that toxicity peaked following 24 hour NMDA exposure. Although NMDA-induced PI fluorescence decreased at later timepoints, PI uptake remained significantly greater than control values. These results largely agree with previous research, which revealed significant increases in PI uptake assessed 1 day or 3 days following NMDA exposure, but not when PI was measured 5 or more days following NMDA exposure (Wilkins et al., 2006). The cytotoxic effect of NMDA was significantly attenuated by the addition of the competitive NMDA receptor antagonist APV, demonstrating that the toxicity observed is indeed dependent on NMDA receptor activation as previously reported (Zimmer et al., 2000; Gibson et al., 2003; Mulholland et al., 2004; Wilkins et al., 2006; Kim et al., 2009; Butler et al., 2010). The present studies extend those previously reported in examining the time course of PI fluorescence during protracted NMDA exposure and identified a time-dependent reduction in PI fluorescence during 120 hours of exposure to NMDA. The decline in PI uptake following extended exposure to NMDA may well reflect phagocytic activity and, hence, reductions in dead or damaged cells. Additionally, excitotoxicity induces increases in deoxyribonuclease, removing the substrate required for PI intercalation (Marti and Fleck, 2004). Similarly, endonuclease G (endoG) is a caspase-independent nuclease found in mitochondria (Li et al., 2001), and during apoptosis, is released from the mitochondria and cleaves chromatin DNA within the nucleus (Li et al., 2001). Previous research has indicated that levels of endoG rise following AMPA-induced excitotoxicity (Henne et al., 2006), an effect which may generalize to all glutamate-induced excitotoxicity. Thus, the time-dependent decline of NMDA-induced PI fluorescence likely reflects catabolic processes initiated by $Ca^{2+}$-dependent signaling with NMDA exposure.

## NMDA-induced loss of synaptophysin

Perhaps the most intriguing finding of the present studies is the marked loss of synaptophysin immunoreactivity in all subregions of the hippocampal formation, including those not demonstrating significant uptake of PI, suggesting a progressive loss of synaptophysin in live cells of the CA3 pyramidal cell layer and DG granule cells, effects prevented by APV co-exposure. We and others have published extensively on the exclusive vulnerability of the CA1 pyramidal cells, rather than CA3 region or DG neurons, to the excitotoxic insults including NMDA exposure and ethanol withdrawal (Prendergast et al., 2001; Butler et al., 2010). However, the present findings may contradict such conclusions. These findings indicate that even though PI incorporation was not observed in CA3 region pyramidal cells or in DG granule cells, synaptic function of what are likely viable neurons is predicted to be compromised. Synaptophysin is likely to be involved in the docking and fusion of the vesicle with the plasma membrane (Sudhof, 1995), possibly via interactions with gamma adaptin (Horikawa et al., 2002), and has been implicated in synaptogenesis and synaptic reorganization (Bergmann et al., 1997). Further, loss of synaptophysin is associated with several forms of neurodegeneration. Notably, synaptophysin is a known substrate of the E3 ubiquitin-protein ligase SIAH2, a member of the seven in abstentia homolog family of proteins (Wheeler et al. 2002), in addition to being a substrate for the proteolytic enzymes mentioned above. It is not known, however, if excitotoxicity induces SIAH2 signaling. Thus, it will be intriguing to further examine the possibility that excitotoxic insult is an inducer of this proteosomal signaling pathway.

## Effect of MDL-28170 on NMDA-induced toxicity and loss of synaptophysin

Further studies were completed to assess the role that cysteine protease, including calpain, activation may have in the cytotoxicity and loss of synaptophysin content associated with prolonged exposure to NMDA. Although previous studies have noted that NMDA receptor antagonism and protease inhibition prevented neurodegeneration both *in vitro* (Nimmrich et al., 2010) and *in vivo* (Granic et al., 2010), no study to date has investigated the effects of cysteine protease inhibition in regards to synaptophysin content with neurodegeneration. Activation of the $Ca^{2+}$-dependent cysteine protease calpain is thought to produce cell death via breakdown of cytoskeletal components other than synaptophysin (Siman and Noszek, 1988; Sattler and Tymianski, 2000). Calpain-mediated cleavage of the membrane cytoskeletal protein spectrin produces orderly break down products following NMDA receptor-mediated excitotoxicity (Bahr et al., 1995; Vanderklish and Bahr, 2000), though it is not clear if synaptophysin is a substrate for calpain and/or other cysteine proteases.

Notably, we observed early sparing of NMDA-induced loss of synaptophysin via blockade of cysteine protease activation using MDL-28170 in all explant subregions. This is the first study, to our knowledge, that demonstrates the time-dependent protective effect of protease inhibition on the loss of synaptophysin produced by an excitotoxic insult. Interestingly, NMDA-induced loss of synaptophysin content was not prevented or even attenuated by MDL-28170 at later time points (120 hours), in any subregion. This finding, in particular, suggests the involvement of cysteine protease-independent mechanisms in the progressive loss of synaptophysin content with prolonged NMDA exposure. This is consistent with findings from hypoxia-ischemia research which suggests that activation of $Ca^{2+}$-dependent calpains can lead to later activation of the apoptotic proteases caspase-3 and caspase-7 (Blomgren et al., 2001; Gafni et al., 2009). Further, sequential activation of calpain, cathepsin-b and caspase-3 has been postulated to occur following ischemic insult in rodent models (Chaitanya and Babu, 2008). It should also be noted that the concentrations of MDL-28170 used in the present set of studies (2.5 and 25 μM) are significantly above the reported $K_I$ value of 10 nM for calpain inhibition (Mehdi, 1991). Although the lower concentration of MDL-28170 used did not provide full protection against the NMDA-induced loss of synaptophysin, 25 μM of MDL-28170 was sufficient to reverse the loss to control levels while not producing toxicity or changes in synaptophysin immunoreactivity alone.

There has been some recent contradiction as to whether synaptophysin may be a substrate for calpains and related cysteine proteases. For example, Thompson and colleagues (2006) revealed activation of calpain-mediated proteolysis, but no changes in synaptophysin levels, following severe controlled cortical impact traumatic brain injury in a rodent model. In contrast, results of the current study suggest that synaptophysin may be a substrate for cysteine proteases, as pharmacologic inhibition of protease activity attenuated the loss of synaptophysin. These results are in agreement with and expand upon previous work by Lee and colleagues (2008) demonstrating that the calpain inhibitor calpeptin attenuated synaptophysin proteolysis at 30 hours following excessive glutamate exposure. Taken together, these results suggest that $Ca^{2+}$-dependent recruitment of cysteine proteases at early timepoints after initiation of excitotoxicity is associated with synaptophysin loss, but activation of alternative signaling effectors with continued exposure to an excitotoxin. The loss of synaptic proteins is a hallmark feature of many neurodegenerative states, including Alzheimer's disease (Honer, 2003), ischemia (Masliah and Terry, 1993), and traumatic brain injury (Ansari et al., 2008). The loss of these proteins may depend on NMDA receptor-mediated $Ca^{2+}$ influx and subsequent activation of pathological isoforms of cysteine proteases (Kelly and Ferreira, 2006). Prevention of early synaptic protein degradation by either NMDA receptor antagonism or targeted cysteine protease inhibition, as observed in the current study, may represent a useful therapeutic tool to treat further neurodegeneration.

Geddes and Saatman (2010) elegantly discuss the role that shRNA or siRNA approaches may have in altering the activation of pathological cysteine protease isoforms in the treatment of neurodegenerative conditions including Huntington's Disease, stroke, and traumatic brain or spinal cord insult. Animal work supports this possibility, in demonstrating that shRNA knockdown of μ-calpain in rat promotes neuronal survival after global cerebral ischemia (Bevers et al. 2010).

## Acknowledgments

## Abbreviations

| | |
|---|---|
| **AMPAr** | α-amino-3-hydroxy-5-methylisoxazole-4-propionic acid receptor |
| **ANOVA** | analysis of variance |
| **APV** | DL-2-Amino-5-phosphonopentanoic acid |
| **CA** | cornu ammonus |
| **Ca$^{2+}$** | calcium |
| **DG** | dentate gyrus |
| **DMSO** | dimethyl sulfoxide |
| **EAA** | excitatory amino acid |
| **endoG** | endonuclease G |
| **FITC** | fluorescein isothiocynate |
| **GluR** | glutamate receptor |
| **MEM** | minimum essential medium |
| **NMDA** | N-methyl-D-aspartate |
| **PBS** | phosphate-buffered saline |
| **PI** | propidium iodide |
| **TBI** | traumatic brain injury |

## References

Ansari MA, Roberts KN, Scheff SW. Oxidative stress and modification of synaptic proteins in hippocampus after traumatic brain injury. Free Radic Biol Med. 2008; 45:443–452. [PubMed: 18501200]

Bahr BA, Tiriveedhi S, Park GY, Lynch G. Induction of calpain-mediated spectrin fragments by pathogenic treatments in long-term hippocampal slices. J Pharmacol Exp Ther. 1995; 273:902–908. [PubMed: 7538583]

Baimbridge KG, Celio MR, Rogers JH. Calcium-binding proteins in the nervous system. Trends Neurosci. 1992; 15:303–308. [PubMed: 1384200]

Bergmann M, Post A, Rittel I, Bechmann I, Nitsch R. Expression of synaptophysin in sprouting neurons after entorhinal lesion in the rat. Exp Brain Res. 1997; 117:80–86. [PubMed: 9386006]

Bevers MB, Ingleton LP, Che D, Cole JT, Li L, Da T, Kopil CM, Cohen AS, Neumar RW. RNAi targeting micro-calpain increases neuron survival and preserves hippocampal function after global brain ischemia. Exp Neurol. 2010; 224:170–177. [PubMed: 20298691]

Blomgren K, Zhu C, Wang X, Karlsson JO, Leverin AL, Bahr BA, Mallard C, Hagberg H. Synergistic activation of caspase-3 by m-calpain after neonatal hypoxia-ischemia: a mechanism of "pathological apoptosis"? J Biol Chem. 2001; 276:10191–10198. [PubMed: 11124942]

Butler TR, Self RL, Smith KJ, Sharrett-Field LJ, Berry JN, Littleton JM, Pauly JR, Mulholland PJ, Prendergast MA. Selective vulnerability of hippocampal cornu ammonis 1 pyramidal cells to excitotoxic insult is associated with the expression of polyamine-sensitive N-methyl-D-asparate-type glutamate receptors. Neuroscience. 2010; 165:525–534. [PubMed: 19837138]

Chaitanya GV, Babu PP. Activation of calpain, cathepsin-b and caspase-3 during transient focal cerebral ischemia in rat model. Neurochem Res. 2008; 33:2178–2186. [PubMed: 18338260]

Choi DW. Excitotoxic cell death. J Neurobiol. 1992; 23:1261–1276. [PubMed: 1361523]

Choi DW. Calcium: still center-stage in hypoxic-ischemic neuronal death. Trends Neurosci. 1995; 18:58–60. [PubMed: 7537408]

Choi DW, Koh JY, Peters S. Pharmacology of glutamate neurotoxicity in cortical cell culture: attenuation by NMDA antagonists. J Neurosci. 1988; 8:185–196. [PubMed: 2892896]

Del Rio P, Montiel T, Massieu L. Contribution of NMDA and non-NMDA receptors to in vivo glutamate-induced calpain activation in the rat striatum. Relation to neuronal damage. Neurochem Res. 2008; 33:1475–1483. [PubMed: 18270815]

Driscoll BF, Deibler GE, Law MJ, Crane AM. Damage to neurons in culture following medium change: role of glutamine and extracellular generation of glutamate. J Neurochem. 1993; 61:1795–1800. [PubMed: 7901333]

Gafni J, Cong X, Chen SF, Gibson BW, Ellerby LM. Calpain-1 cleaves and activates caspase-7. J Biol Chem. 2009; 284:25441–25449. [PubMed: 19617626]

Geddes JW, Saatman KK. Targeting individual calpain isoforms for neuroprotection. Exp Neurol. 2010; 226:6–7. [PubMed: 20682310]

Gellerman DM, Bi X, Baudry M. NMDA receptor-mediated regulation of AMPA receptor properties in organotypic hippocampal slice cultures. J Neurochem. 1997; 69:131–136. [PubMed: 9202303]

Gibson DA, Harris BR, Prendergast MA, Hart SR, Blanchard JA 2nd, Holley RC, Pedigo NW, Littleton JM. Polyamines contribute to ethanol withdrawal-induced neurotoxicity in rat hippocampal slice cultures through interactions with the NMDA receptor. Alcohol Clin Exp Res. 2003; 27:1099–1106. [PubMed: 12878916]

Granic I, Nyakas C, Luiten PG, Eisel UL, Halmy LG, Gross G, Schoemaker H, Moller A, Nimmrich V. Calpain inhibition prevents amyloid-beta-induced neurodegeneration and associated behavioral dysfunction in rats. Neuropharmacology. 2010; 59:334–342. [PubMed: 20650285]

Gutierrez R, Heinemann U. Synaptic reorganization in explanted cultures of rat hippocampus. Brain Res. 1999; 815:304–316. [PubMed: 9878801]

Henne WM, Oomman S, Attridge J, Finckbone V, Coates P, Bliss R, Strahlendorf H, Strahlendorf J. AMPA-induced excitotoxicity increases nuclear levels of CAD, endonuclease G, and acinus and induces chromatin condensation in rat hippocampal pyramidal neurons. Cell Mol Neurobiol. 2006; 26:321–339. [PubMed: 16767516]

Honer WG. Pathology of presynaptic proteins in Alzheimer's disease: more than simple loss of terminals. Neurobiol Aging. 2003; 24:1047–1062. [PubMed: 14643376]

Horikawa HP, Kneussel M, El Far O, Betz H. Interaction of synaptophysin with the AP-1 adaptor protein gamma-adaptin. Mol Cell Neurosci. 2002; 21:454–462. [PubMed: 12498786]

Hou ST, Jiang SX, Aylsworth A, Ferguson G, Slinn J, Hu H, Leung T, Kappler J, Kaibuchi K. CaMKII phosphorylates collapsin response mediator protein 2 and modulates axonal damage during glutamate excitotoxicity. J Neurochem. 2009; 111:870–881. [PubMed: 19735446]

Kelly BL, Ferreira A. beta-Amyloid-induced dynamin 1 degradation is mediated by N-methyl-D-aspartate receptors in hippocampal neurons. J Biol Chem. 2006; 281:28079–28089. [PubMed: 16864575]

Kim HW, Chang YC, Chen M, Rapoport SI, Rao JS. Chronic NMDA administration to rats increases brain pro-apoptotic factors while decreasing anti-Apoptotic factors and causes cell death. BMC Neurosci. 2009; 10:123. [PubMed: 19785755]

Lee JH, Lee EO, Kang JL, Chong YH. Concomitant degradation of beta-catenin and GSK-3 beta potently contributes to glutamate-induced neurotoxicity in rat hippocampal slice cultures. J Neurochem. 2008; 106:1066–1077. [PubMed: 18445133]

Li LY, Luo X, Wang X. Endonuclease G is an apoptotic DNase when released from mitochondria. Nature. 2001; 412:95–99. [PubMed: 11452314]

Martens U, Wree A. Distribution of [3H]MK-801, [3H]AMPA and [3H]Kainate binding sites in rat hippocampal long-term slice cultures isolated from external afferents. Anat Embryol (Berl). 2001; 203:491–500. [PubMed: 11453166]

Marti TM, Fleck O. DNA repair nucleases. Cell Mol Life Sci. 2004; 61:336–354. [PubMed: 14770297]

Masliah E, Terry R. The role of synaptic proteins in the pathogenesis of disorders of the central nervous system. Brain Pathol. 1993; 3:77–85. [PubMed: 8269086]

Mayer S, Harris B, Gibson DA, Blanchard J, Prendergast MA, Holley RC, Littleton J. Acamprosate has no effect on NMDA-induced toxicity but reduces toxicity induced by spermidine or by changing the medium in organotypic hippocampal slice cultures from rat. Alcohol Clin Exp Res. 2002; 26:655–662. [PubMed: 12045473]

Mehdi S. Cell-penetrating inhibitors of calpain. Trends Biochem Sci. 1991; 16:150–153. [PubMed: 1877091]

Mulholland PJ, Prendergast MA. Transection of intrinsic polysynaptic pathways reduces N-methyl-D-aspartate neurotoxicity in hippocampal slice cultures. Neurosci Res. 2003; 46:369–376. [PubMed: 12804798]

Mulholland PJ, Self RL, Harris BR, Littleton JM, Prendergast MA. (-)-nicotine ameliorates corticosterone's potentiation of N-methyl-d-aspartate receptor-mediated cornu ammonis 1 toxicity. Neuroscience. 2004; 125:671–682. [PubMed: 15099681]

Nimmrich V, Reymann KG, Strassburger M, Schoder UH, Gross G, Hahn A, Schoemaker H, Wicke K, Moller A. Inhibition of calpain prevents NMDA-induced cell death and beta-amyloid-induced synaptic dysfunction in hippocampal slice cultures. Br J Pharmacol. 2010; 159:1523–1531. [PubMed: 20233208]

Pivovarova NB, Andrews SB. Calcium-dependent mitochondrial function and dysfunction in neurons. FEBS J. 2010; 277:3622–3636. [PubMed: 20659161]

Prendergast MA, Harris BR, Mayer S, Holley RC, Hauser KF, Littleton JM. Chronic nicotine exposure reduces N-methyl-D-aspartate receptor-mediated damage in the hippocampus without altering calcium accumulation or extrusion: evidence of calbindin-D28K overexpression. Neuroscience. 2001; 102:75–85. [PubMed: 11226671]

Prendergast MA, Harris BR, Mullholland PJ, Blanchard JA 2nd, Gibson DA, Holley RC, Littleton JM. Hippocampal CA1 region neurodegeneration produced by ethanol withdrawal requires activation of intrinsic polysynaptic hippocampal pathways and function of N-methyl-D-aspartate receptors. Neuroscience. 2004; 124:869–877. [PubMed: 15026127]

Rami A, Ferger D, Krieglstein J. Blockade of calpain proteolytic activity rescues neurons from glutamate excitotoxicity. Neurosci Res. 1997; 27:93–97. [PubMed: 9089703]

Sattler R, Tymianski M. Molecular mechanisms of calcium-dependent excitotoxicity. J Mol Med. 2000; 78:3–13. [PubMed: 10759025]

Siman R, Noszek JC. Excitatory amino acids activate calpain I and induce structural protein breakdown in vivo. Neuron. 1988; 1:279–287. [PubMed: 2856162]

Siman R, Noszek JC, Kegerise C. Calpain I activation is specifically related to excitatory amino acid induction of hippocampal damage. J Neurosci. 1989; 9:1579–1590. [PubMed: 2542478]

Stroemer RP, Kent TA, Hulsebosch CE. Neocortical neural sprouting, synaptogenesis, and behavioral recovery after neocortical infarction in rats. Stroke. 1995; 26:2135–2144. [PubMed: 7482662]

Sudhof TC. The synaptic vesicle cycle: a cascade of protein-protein interactions. Nature. 1995; 375:645–653. [PubMed: 7791897]

Thompson SN, Gibson TR, Thompson BM, Deng Y, Hall ED. Relationship of calpain-mediated proteolysis to the expression of axonal and synaptic plasticity markers following traumatic brain injury in mice. Exp Neurol. 2006; 201:253–265. [PubMed: 16814284]

Vanderklish PW, Bahr BA. The pathogenic activation of calpain: a marker and mediator of cellular toxicity and disease states. Int J Exp Pathol. 2000; 81:323–339. [PubMed: 11168679]

Vosler PS, Brennan CS, Chen J. Calpain-mediated signaling mechanisms in neuronal injury and neurodegeneration. Mol Neurobiol. 2008; 38:78–100. [PubMed: 18686046]

Wiedenmann B, Franke WW. Identification and localization of synaptophysin, an integral membrane glycoprotein of Mr 38,000 characteristic of presynaptic vesicles. Cell. 1985; 41:1017–1028. [PubMed: 3924408]

Wilkins LH Jr, Prendergast MA, Blanchard J, Holley RC, Chambers ER, Littleton JM. Potential value of changes in cell markers in organotypic hippocampal cultures associated with chronic EtOH exposure and withdrawal: comparison with NMDA-induced changes. Alcohol Clin Exp Res. 2006; 30:1768–1780. [PubMed: 17010144]

Zimmer J, Kristensen BW, Jakobsen B, Noraberg J. Excitatory amino acid neurotoxicity and modulation of glutamate receptor expression in organotypic brain slice cultures. Amino Acids. 2000; 19:7–21. [PubMed: 11026469]

## Highlights

Density of the synaptic vesicle protein synaptophysin increases with in vitro aging

Synaptophysin content was reduced in cell layers not demonstrating neuronal injury.

Cysteine protease activation is temporally limited following excitotoxicity
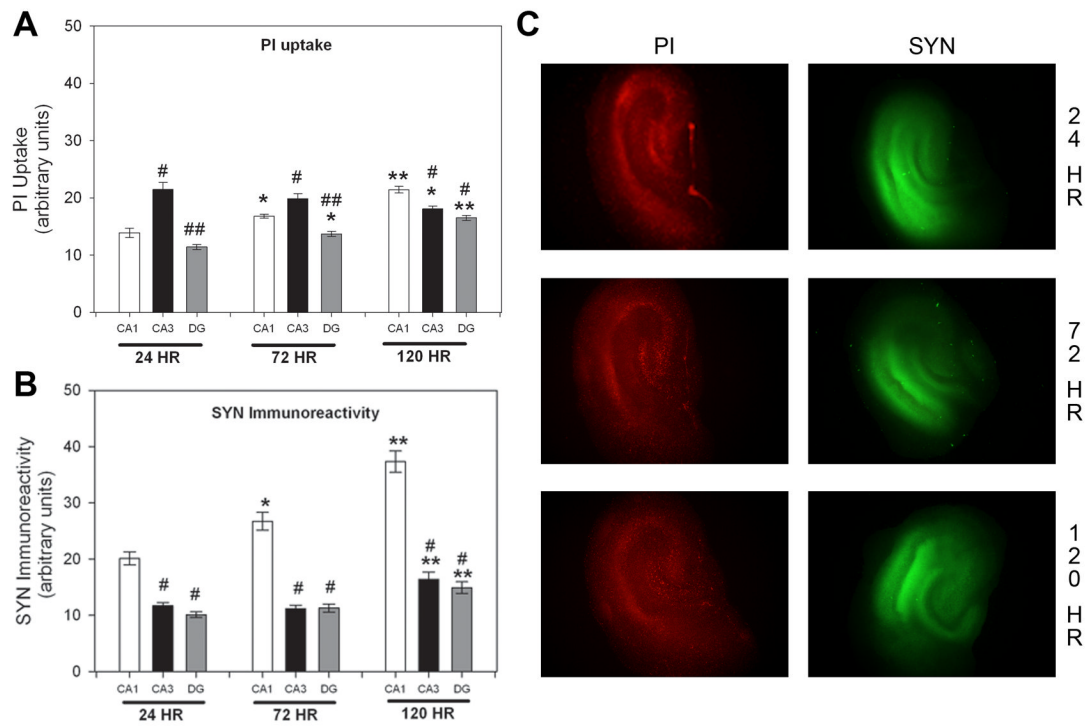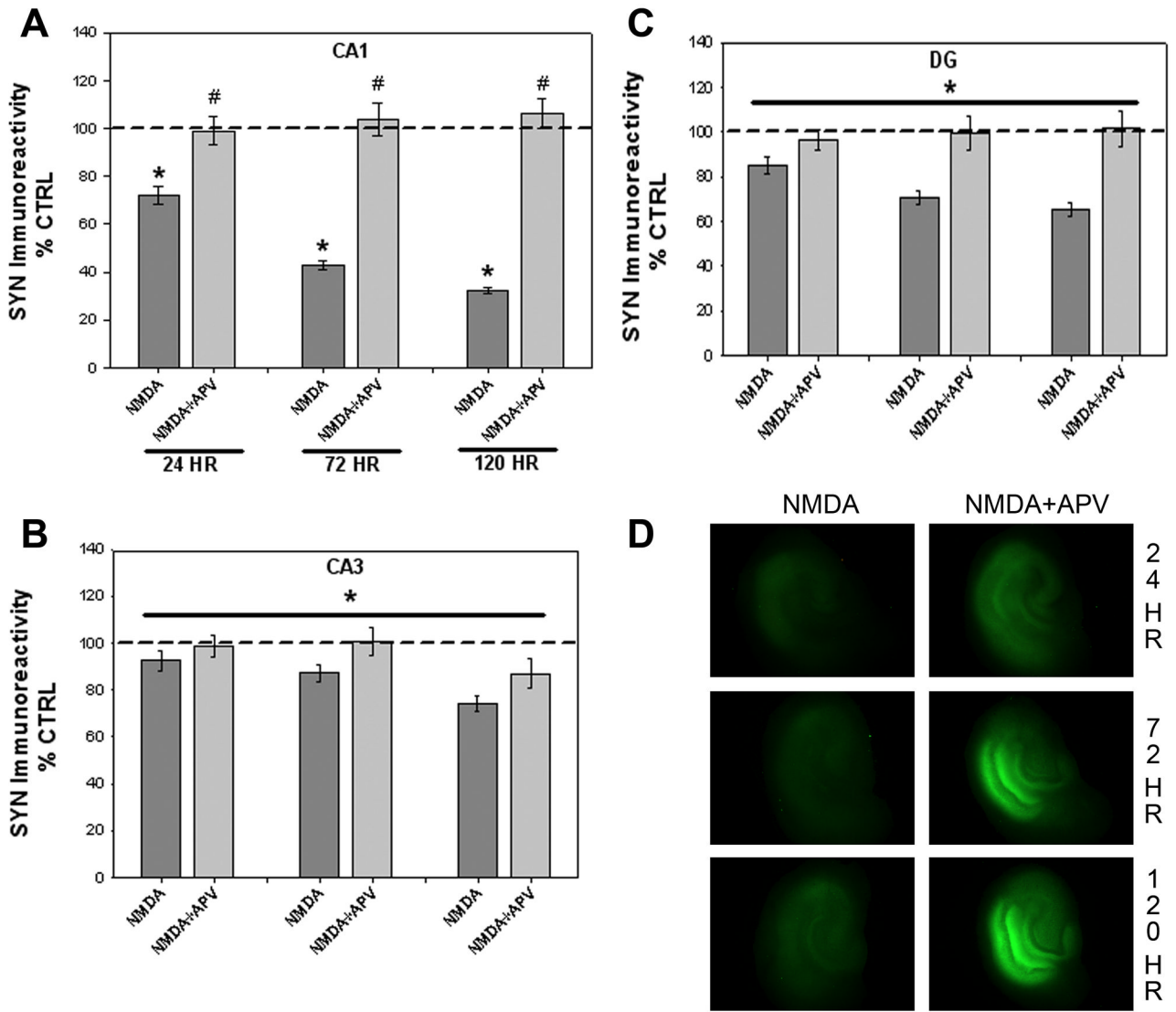
**Figure 1.**
PI uptake in control slices was compared in each hippocampal region for each timepoint **(A)**, as was synaptophysin (SYN) immunoreactivity **(B)**. * $p<0.05$ vs. 24 hour within region; ** $p<0.05$ vs. 72 hour and 24 hour within region; # $p<0.05$ vs. CA1 region within time; ## $p<0.05$ vs. CA1 and CA3 regions within time **(C)** Representative images of PI and SYN fluorescence in control hippocampal slices
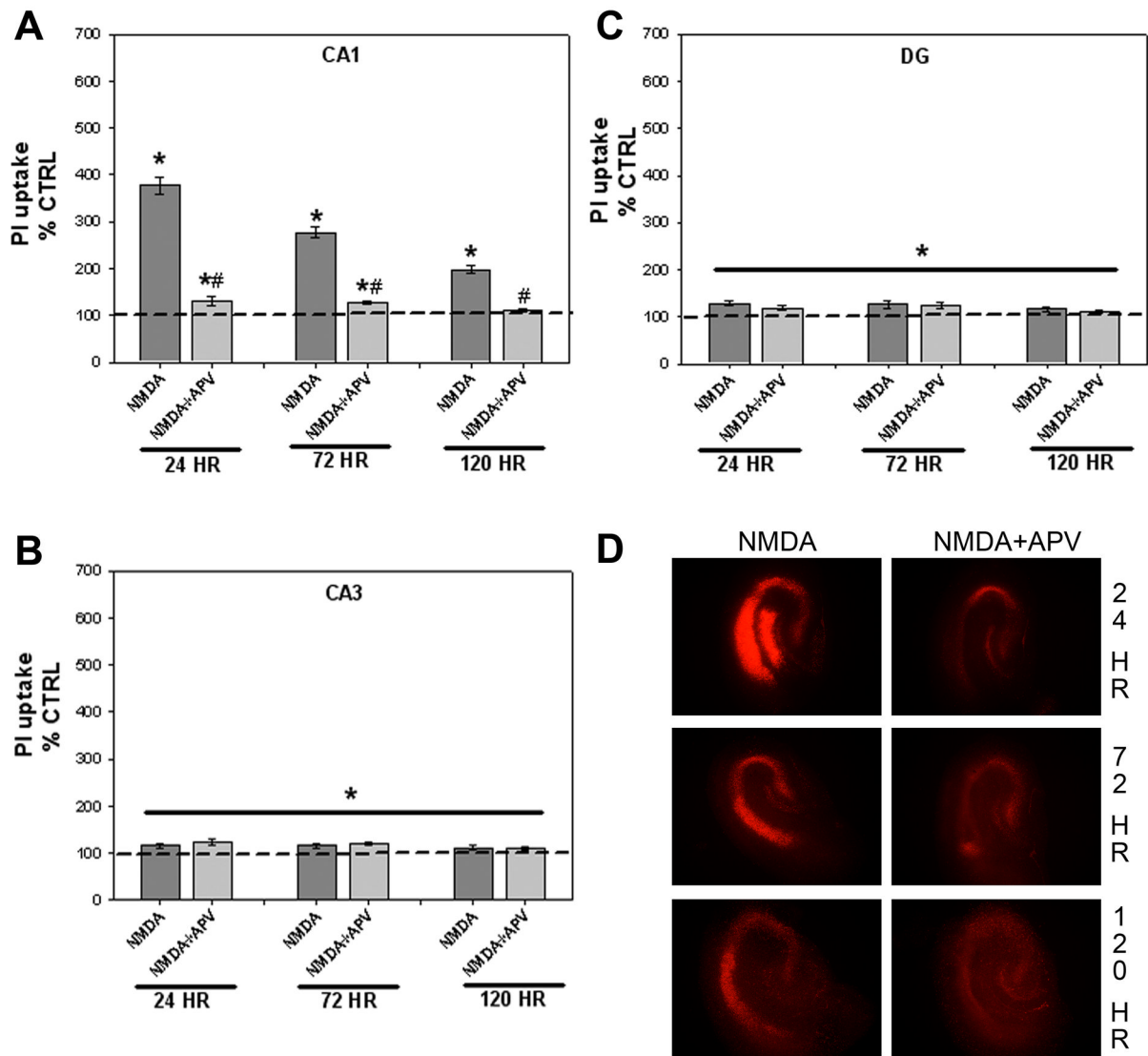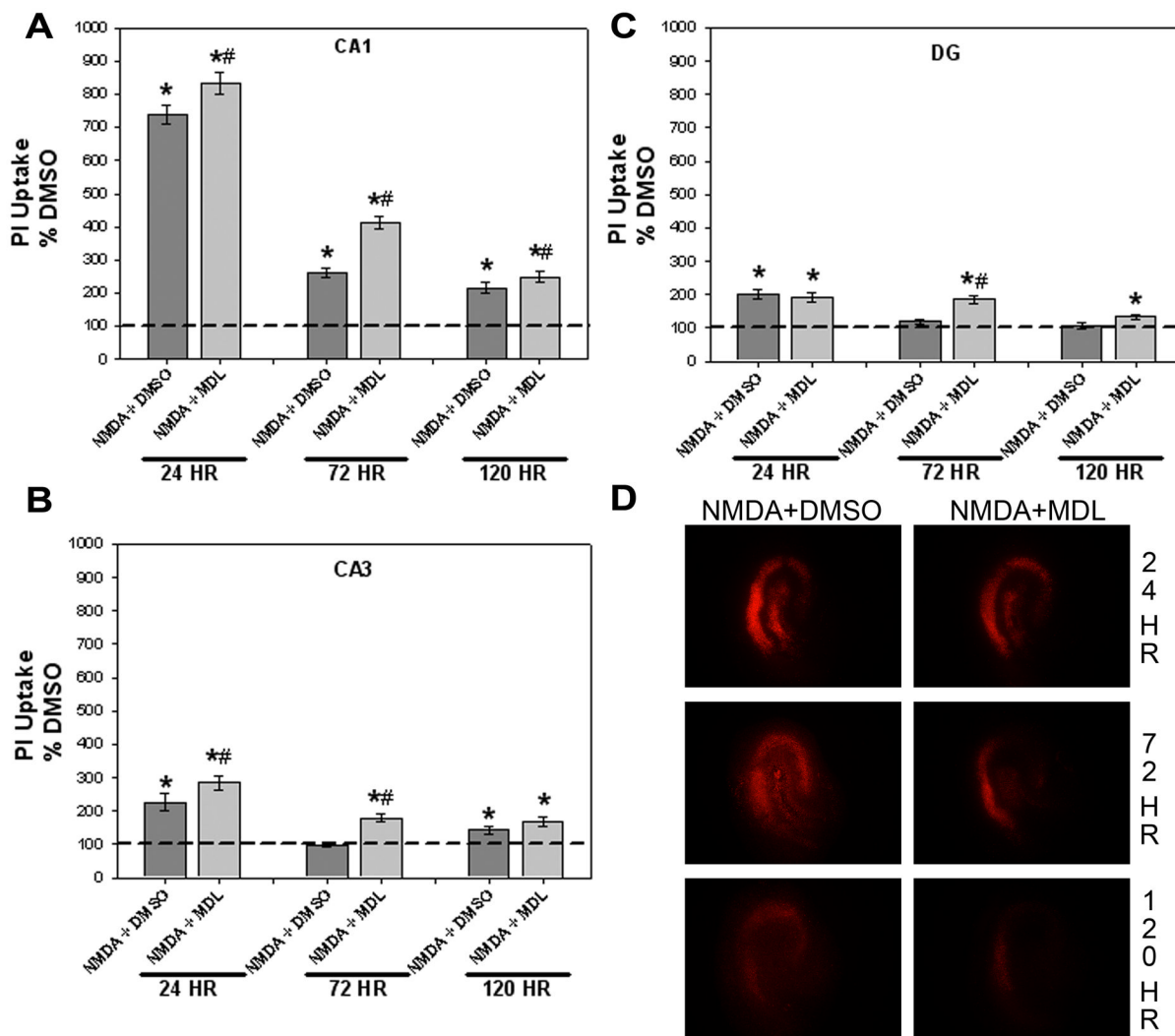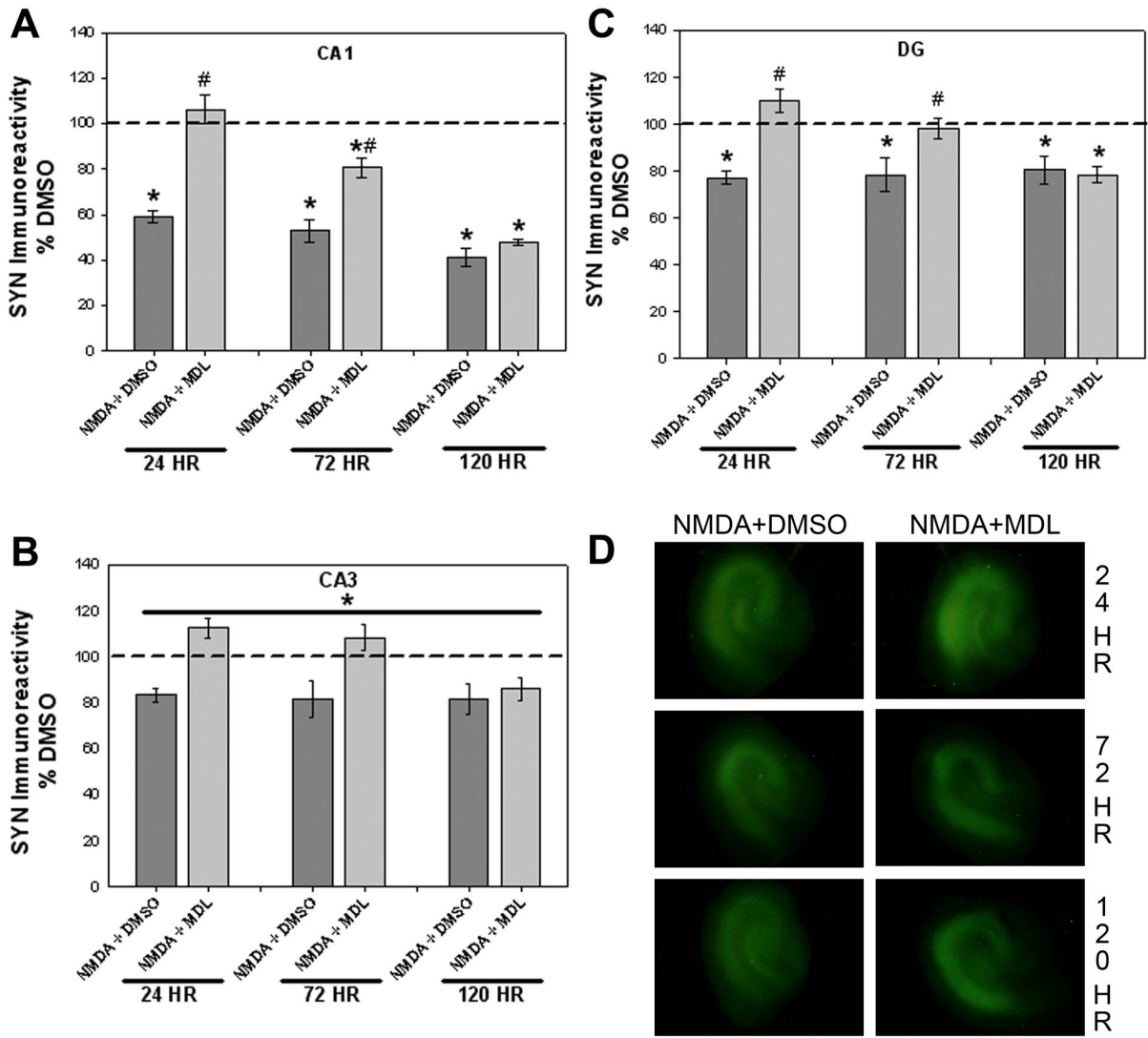
**Figure 2.**
Effects of exposure to the glutamate NMDA receptor agonist NMDA or co-exposure to NMDA and the competitive antagonist APV on toxicity observed in the organotypic hippocampal slice cultures. Exposure to NMDA resulted in significant time-dependent toxicity within the CA1 region of the hippocampus **(A)**, an effect which was prevented by co-exposure to APV. Collapsed across time, exposure to NMDA also resulted in significant toxicity in the CA3 **(B)** and DG **(C)** regions of the hippocampus. * $p < 0.05$ vs. control levels; # $p < 0.05$ vs. NMDA alone. **(D)** Representative images of PI uptake in hippocampal slices treated with NMDA or NMDA+APV

**Figure 3.**
Effects of exposure to the glutamate NMDA receptor agonist NMDA or co-exposure to NMDA and the competitive antagonist APV on immunoreactivity for the synaptic vesicle protein synaptophysin (SYN) observed in the organotypic hippocampal slice cultures. **(A)** Exposure to NMDA resulted in significant time-dependent synaptophysin loss within the CA1 region of the hippocampus, an effect which was prevented by co-exposure to APV. Collapsed across time, NMDA exposure resulted in significant decreased synaptophysin immunoreactivity within the CA3 **(B)** and DG **(C)** regions of the hippocampus. * $p<0.05$ vs. control levels; # $p<0.05$ vs. NMDA alone. **(D)** Representative images of immunoreactivity for synaptophysin in hippocampal slices treated with NMDA or NMDA+APV

**Figure 4.**
Effects of co-exposure to NMDA and either DMSO (vehicle) or the cysteine protease inhibitor MDL-28170 (25 μM) on toxicity observed in the organotypic hippocampal slice cultures. Co-exposure to NMDA+DMSO resulted in significant time-dependent toxicity within the CA1 **(A)**, CA3 **(B)** and DG **(C)** regions of the hippocampus while co-exposure to MDL-28170 did not attenuate NMDA-induced toxicity. * $p < 0.05$ vs. DMSO (vehicle) levels; # $p < 0.05$ vs. NMDA+DMSO. **(D)** Representative images of PI uptake in hippocampal slices treated with NMDA+DMSO or NMDA+MDL

**Figure 5.**
Effects of co-exposure to NMDA and either DMSO (vehicle) or the cysteine protease inhibitor MDL-28170 (25 µM) on the synaptic vesicle protein synaptophysin (SYN) immunoreactivity observed in the organotypic hippocampal slice cultures. Co-exposure to NMDA+DMSO resulted in significant time-dependent loss of synaptophysin within the pyramidal cell layer of the CA1 **(A)**, an effect which was prevented by co-exposure to MDL-28170 at 24 and 72 hours. Collapsed across time, NMDA+DMSO exposure resulted in significant decreased synaptophysin immunoreactivity within the CA3 region **(B)**, which was also prevented by co-exposure to MDL-28170. As with the CA1, co-exposure to NMDA+DMSO resulted in a significant time-dependent loss of synaptophysin immunoreactivity in the granule cell layer of the DG **(C)**, an effect which was prevented by co-exposure to MDL-28170 at 24 or 72 hours. * $p<0.05$ vs. DMSO (vehicle) levels; # $p<0.05$ vs. NMDA+DMSO. **(D)** Representative images of immunoreactivity for synaptophysin in hippocampal slices treated with NMDA+DMSO or NMDA+MDL

**Table 1**

Effects of co-exposure to NMDA (20 µM) and either DMSO (vehicle) or the cysteine protease inhibitor MDL-28170 (2.5 µM) on PI uptake and synaptophysin (SYN) immunoreactivity at 24 hours. Co-exposure to NMDA+DMSO resulted in significant toxicity within each region of the hippocampus examined, while co-exposure to MDL-28170 (2.5 µM) had no effect on NMDA-induced toxicity. Co-exposure to NMDA+DMSO resulted in a significant loss of synaptophysin immunoreactivity within the pyramidal cell layer of the CA1 and the granule cell layer of the DG, an effect which was significantly attenuated by co-exposure to MDL-28170 (2.5 µM).

| PI Uptake | CA1 ± SEM | CA3 ± SEM | DG ± SEM |
|---|---|---|---|
| NMDA + DMSO | *828.762 ± 47.833 | *230.517 ± 29.551 | *250.452 ± 24.941 |
| NMDA + MDL 2.5 | *833.467 ± 41.976 | *243.893 ± 25.006 | *220.853 ± 21.742 |

| SYN Immunoreactivity | CA1 ± SEM | CA3 ± SEM | DG ± SEM |
|---|---|---|---|
| NMDA + DMSO | *73.932 ± 3.018 | 86.133 ± 4.389 | *84.365 ± 3.670 |
| NMDA + MDL 2.5 | #92.749 ± 3.034 | #107.226 ± 5.731 | #99.623 ± 4.558 |

*
p<0.05 vs. DMSO (vehicle) levels;

#
p<0.05 vs. NMDA+DMSO.